Nanotechnology

TOPICAL REVIEW

Enhancing conversion efficiency in Si-based hybrid photovoltaic-thermoelectric solar cells

Dario Narducci*, Federico Giulio and Antonio Mazzacua

Department of Materials Science, University of Milano Bicocca, Milan, Italy
* Author to whom any correspondence should be addressed.

E-mail: dario.narducci@unimib.it

Keywords: solar harvesting, thermoelectricity, photovoltaics, silicon

OPEN ACCESS

RECEIVED
27 January 2026

REVISED
9 April 2026

ACCEPTED FOR PUBLICATION
18 May 2026

PUBLISHED
1 June 2026

Abstract

Photovoltaic (PV) solar cells play a central role among renewable energy sources, which currently account for 33% of electric power generation worldwide. PV cell efficiency is known to be limited by their incapability of converting the portion of the solar spectrum whose energy is lower than the PV material energy gap. However, such low-frequency part of the solar spectrum can be converted into heat and then, in turn, transformed into electric power by thermoelectric generators (TEGs). Considering that 90% of PV modules are based on Si, either single-crystalline or polycrystalline, the development of Si-based hybrid solar harvesters with enhanced conversion efficiencies would provide a remarkable contribution to the overall renewable power generation. This review will analyse recent advancements in the PV-TEG hybridisation focusing on Si-based PV cells at low solar concentration. Two well-established approaches will be mainly discussed, namely tandem hybridization, where TEGs are in a thermal series with the PV cell, and spectral-split hybridization, where instead suitable optics splits the solar spectrum, conveying its high-frequency part to the PV cell and the remaining part toward the TEG. Account will be given to both energetic and economic profitability, elaborating on the strategies to evade physical and economic constraints that are still limiting the exploitation of such technologies in the most relevant and diffused class of solar harvesters.

1. Introduction

Over the last decades, the search for alternate power sources replacing fossil resources has intensified. While hydroelectricity still retains the largest share, electric energy produced by photovoltaic (PV) modules has increased from 0.65% in 2015 to 8.67% in 2025 [1]. Remarkably, *distributed* PV generation currently covers about 45% of the total PV power [1], with about 90% of PV modules being based on Si, either single-crystalline or polycrystalline [2]. Also motivated by its large dominance on the PV market, efficiency of PV cells has increased from 25% in 2000 to the world-best 27.8% in 2025 [3], approaching the Shockley–Queisser limit (32%) [4]. Thus, as of today, Si-based PV *modules* display efficiencies of about 22% at 1 Sun (no optical concentration) [5].

Physics of PV generation limits conversion efficiency due to the unused portion of the solar spectrum, as photons with energies lower that the PV materials energy gap E_g are not absorbed and converted. Furthermore, the thermalisation of hot hole–electron pairs additionally reduces efficiency, partially back-converting electric power into heat. This has elicited the idea of pairing PV cells to thermoelectric generators (TEGs), converting heat generated by the PV cell and therefore increasing the overall solar conversion efficiency. Various strategies have been considered, all of them attempting to avoid the shortcomings due to the opposite temperature requirements of PV cells, whose efficiency decreases with the temperature, and of TEGs, needing instead a relatively large temperature difference across the device. Such opposition is very critical for Si cells, whose efficiency coefficient of temperature is especially large. In this review we will analyse how hybridisation can be implemented in Si-based hybrid PV-thermoelectric (TE) generators. Reviews were recently published on the hybridisation of large-gap PV

materials [6–8], multi-junction solar cells [9], and perovskite-based PV cells [10]. Instead, no critical review on Si-based hybrid harvesters has been published lately, despite the fact that hybridisation of Si PVs has the potential to leverage the technology of paired PV-TE solar harvesting.

This review is organised as follows. Section 2 will recall the basic physics ruling PV and TEG efficiency. Ways of pairing PV cells and TEGs will be presented and discussed in section 3. Energetic profitability of hybrid harvesters will be covered in section 4 while their economic convenience will be discussed in section 5, in both cases with a focus on Si-based PV cells. A view of possible research directions will be finally presented in section 6.

2. Conversion efficiencies

2.1. Single-junction PV cell efficiency

The *maximum* efficiency of a single-junction solar cells is ruled by the Shockley–Queisser (SQ) model, which assumes the radiative recombination as the only hole–electron recombination mechanism limiting PV cell conversion rate. In such limit, maximum power generation follows by computing the PV current density J_{PV} as the balance between adsorbed and emitted photon rates, namely

$$J_{PV} = q\left(n_{abs} - n_{emit}\right) \tag{1}$$

where $-q$ is the electron charge. Since PV cells absorb photons from a small angle Ω_{abs} while re-emitting them in a much broader solid angle Ω_{emit}, then

$$n_{abs} = \frac{2\Omega_{abs}}{c^2h^3}\int_{E_g}^{\infty}\frac{E^2}{\exp\left(\dfrac{E}{k_BT_s}\right)-1}\mathrm{d}E \tag{2}$$

where we assumed that Sun radiates as a black-body and c, h and k_B are the speed of light, the Planck's and the Boltzmann's constants while T_s is the Sun temperature. Instead, the emitted photon rate by radiative recombination must consider that the chemical potential of the electron–hole pairs equals qV_{PV}, where V_{PV} is the voltage across the PV cell. Therefore

$$n_{emit} = \frac{2\Omega_{emit}}{c^2h^3}\int_{E_g}^{\infty}\frac{E^2}{\exp\left(\dfrac{E-qV_{PV}}{k_BT_{PV}}\right)-1}\mathrm{d}E \tag{3}$$

where T_{PV} is the cell temperature. Since n_{emit} increases with V_{PV} (and therefore J_{PV} decreases with it), the maximum power output occurs at an intermediate cell voltage. Also note that J_{PV} scales with the $\Omega_{abs}/\Omega_{emit}$. Since Ω_{abs} increases upon optical concentration (linearly, when a point-focused mirror is used), an increase of efficiency with optical concentration is anticipated. In the Boltzmann approximation [11], replacing equations (2) and (3) into equation (1), current density reads

$$J_{PV} = \frac{2q}{c^2h^3}\left(\mathrm{e}^{-E_g/k_BT_s}k_BT_s\left(E_g^2+2E_gk_BT_s+2k_B^2T_s^2\right)\Omega_{abs}\right. \tag{3}$$

$$\left.-\mathrm{e}^{-\left(E_g+qV_{PV}\right)/k_BT_{PV}}k_BT_{PV}\left(E_g^2+2E_gk_BT_{PV}+2k_B^2T_{PV}^2\right)\Omega_{emit}\right) \tag{4}$$

Since $E_g^2 \gg 2E_gk_BT_s+2k_B^2T_s^2$, maximum over V_{PV} of the output power density $w_{PV} = J_{PV}V_{PV}$ simplifies to

$$w_{PV} = \frac{k_B^2T_{PV}T_s\Omega_{abs}E_g^2\left(1-2\mathcal{W}(\phi)\right)^2}{2c^2h^3\mathcal{W}(\phi)}\mathrm{e}^{-E_g/k_BT_s} \tag{5}$$

where $\mathcal{W}$ is the Lambert function and

$$\phi = \frac{T_s\Omega_{abs}}{2T_{PV}\Omega_{emit}}\exp\left(\frac{1}{2}+E_g\left(\frac{1}{k_BT_{PV}}-\frac{1}{k_BT_s}\right)\right) \tag{6}$$

Notably, detailed balance analysis along with equation (3) reports a first dependence of the conversion rate on the cell temperature. Since n_{emit} increases with T_{PV}, efficiency decreases with increasing T_{PV}.

A fundamental factor impacting efficiency that is not encompassed in the SQ model is the dependence of the energy gap on the temperature. Although seemingly small in the temperature range of practical importance for PV cells (for Si, $\mathrm{d}E_g/\mathrm{d}T = -0.27$ meV/K, causing a change of the energy gap

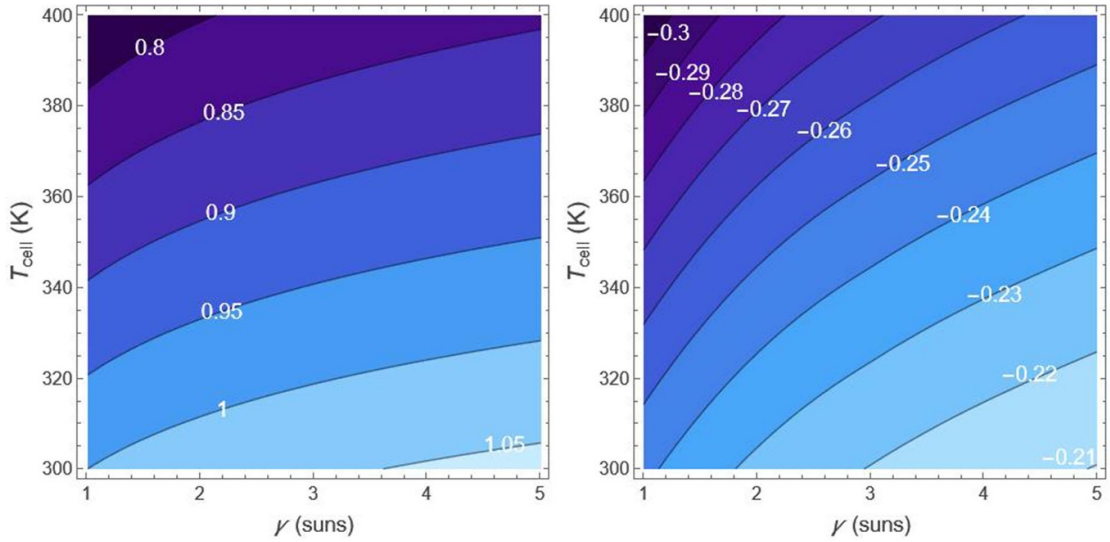

Figure 1. Dependence on temperature and optical concentration for $E_g = 1.12$ eV, ERE = 0.01, of (a) SQ efficiency, normalized to its value at 298 K, 1 Sun; and (b) coefficient of temperature of the SQ efficiency (%/K).

of about 1% over 50 K), it was shown [12] to lead to a decrease of ≈ 4% of the SQ efficiency in most PV cells of practical relevance when T_{PV} increases from 25 to 85 °C. Figure 1 shows the computed value of the temperature coefficient of the PV efficiency $\beta(T_{PV}, \gamma) = \eta_{PV}^{-1} \partial \eta_{PV} / \partial T_{PV}$ for Si (E_g(298 K) = 1.12 eV), based on the SQ model. A value of −0.238%/K at 298 K and one Sun is found [13].

Real-world efficiency of a PV cell (and, even more, of a PV module) is much lower, however, because of additional losses due to non-radiative recombination mechanisms, including Shockley–Read–Hall, Auger and surface recombination, and to cell design (reflection at cell front surface, electrical shunts, Joule dissipation and contact resistances). They also remarkably increases β_{PV} upon cell heating.

With the exception of front cell photon reflection, each of them causes back-conversion of electric power into heat, with losses depending in turn on cell temperature. It is customary [13] to split the coefficient of temperature of PV efficiency β_{PV} into three components, namely $\beta_x = x^{-1} \partial x / \partial T$ where $x = V_{oc}, J_{sc}$, FF, with FF being the fill factor. A detailed analysis of all losses is extremely complicated and only parametric empirical models are currently available. We choose here to use the concept of external radiative efficiency (ERE), introduced by Green [14] and defined as the fraction of the total dark current recombination in the device that results in radiative emission from the device itself, thus correlating the efficiency of a PV cell with that predicted by the SQ model. In practical terms, since ERE encompasses all non-radiative recombination mechanisms, it mostly measures materials quality (defects). Thus, it may be conveniently used to estimate the overall loss of efficiency due to the technological maturity of a PV material and of the cell technology, independently of the PV material—with ERE up to $\approx 10^{-2}$ for single-crystalline Si.

It can be shown [12] that the open-circuit voltage V_{oc} in the presence of non-radiative recombination reads

$$V_{oc}(\mathrm{ERE}) = V_{oc,SQ} + \frac{k_B T_{PV}}{q} \ln(\gamma \mathrm{ERE}) \tag{7}$$

where $V_{oc,SQ}$ is the V_{oc} in the radiative recombination limit at 1 Sun and γ is the optical concentration. Instead, the short-circuit current density is related to its radiative limit J_{SQ} as [15, 16]

$$J_{sc} = q \left(\gamma \Phi_{above}(E_g) - \frac{r_0(E_g, T_{PV})}{\mathrm{ERE}} \right) \tag{8}$$

(where $\Phi_{above}(E_g)$ is the flux of incident photon with energy larger that E_g) where the radiative recombination rate is given by

$$r_0(E_g, T_{PV}) = \frac{2\pi}{c^2 h^3} \int_{E_g}^{\infty} \frac{E^2}{\exp\left(\frac{E}{k_B T_{PV}}\right) - 1}. \tag{9}$$

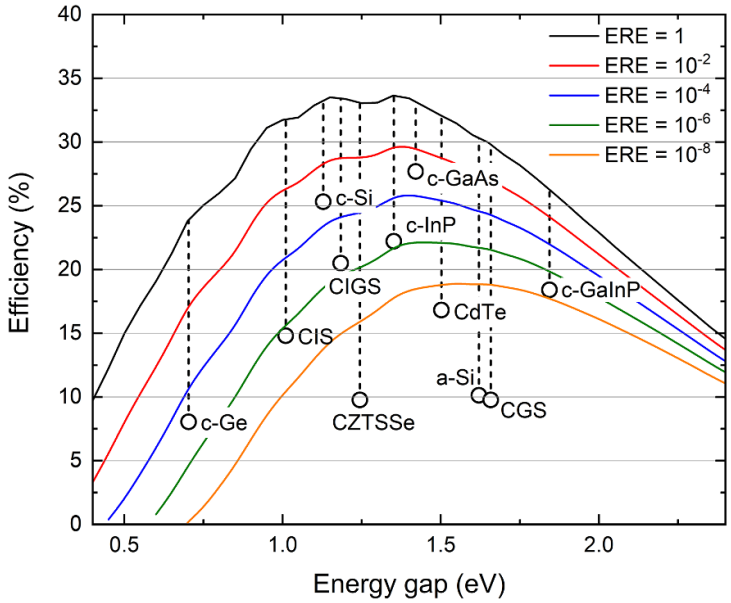

Figure 2. Efficiencies of PV cells as a function of their energy gap and of their ERE. Maximum projected efficiencies for each material are shown by the ERE = 1 curve. Adapted from [16]. CC BY 4.0.

Furthermore, the fill factor depends on ERE according to the approximated formula

$$\mathrm{FF}\left(\mathrm{ERE}\right)=\frac{v_{\mathrm{oc}}\left(\mathrm{ERE}\right)-\ln\left(v_{\mathrm{oc}}\left(\mathrm{ERE}\right)+0.72\right)}{v_{\mathrm{oc}}\left(\mathrm{ERE}\right)+1} \tag{10}$$

where $v_{\mathrm{oc}}(\mathrm{ERE})=qV_{\mathrm{oc}}(\mathrm{ERE})/(k_{\mathrm{B}}T)$. Maximum efficiency reads then

$$\eta_{\mathrm{PV}}\left(\mathrm{ERE}\right)=\frac{\gamma n_{\mathrm{abs}}k_{\mathrm{B}}T_{\mathrm{PV}}\left(2\mathcal{W}\left(z\right)-1\right)^{2}}{\gamma G\mathcal{W}\left(z\right)} \tag{11}$$

where G is the Sun integrated irradiance and $z=2.718\gamma\mathrm{ERE}n_{\mathrm{abs}}/r_0$. Figure 2 displays the efficiency of PV materials as a function of their E_{g} and ERE [16].

Manifestly enough, PV cell temperature also depends on how heat is exchanged with the surroundings. In most PV modules, heat is withdrawn radiatively and convectively, both from the top and the bottom of the module. This makes T_{PV} also dependent on the module mounting, the materials used in the top and bottom layers, and on the way the cell is encapsulated. Additionally, the possible use of spontaneous or forced convective heat exchangers sets the total thermal transfer coefficient h_{HX} toward the surroundings.

2.2. Efficiency of TEGs

TEGs are devices capable of partially converting heat fluxes into electric power due to the possibility of eliciting a current density by applying a temperature difference across a medium. Irreversible thermodynamics teaches that heat fluxes J_{q} and current densities J depend on the gradient of the temperature ∇T and on the electric field $\vec{\mathcal{E}}$ as

$$\begin{aligned}\vec{J}_{\mathrm{q}} &= -\kappa\nabla T+\alpha\sigma_T T\vec{\mathcal{E}}\\ \vec{J} &= -\alpha\sigma_T\nabla T+\sigma_T\vec{\mathcal{E}}\end{aligned} \tag{12}$$

where σ_T is the isothermal electrical conductivity, κ the thermal conductivity, and α the Seebeck coefficient [17]. Since conversion of heat into electric power is due to charge carriers diffusing across the medium because of the thermal gradient, conversion rate increases with σ_T (low electrical resistance opposing to diffusion) and with α, ruling the electric field felt by carriers. On the opposite, a low κ is preferred, since it would limit the heat lost by thermal conduction, which largely prevails (except for metals) on the convective (charge-carrier borne) heat transport mechanism. Thus, assuming that all transport coefficients σ_T, α, and κ are constant over the temperature range the device operates across (constant-property approximation, CPA), one finds that the TEG *efficiencies* depend on the so-called TE figure of merit $zT\equiv\sigma_T\alpha^2T/\kappa$.

Differently from PV cells, where the radiative power input is externally set, TEG operation may take place by setting either the temperature drop across the device or the input heat flux [17]. Thus, since in any heat engine the efficiency is the ratio between the generated work (power) and the input heat (heat current), two optima are defined, namely the maximum efficiency $\eta_{\mathrm{TEG,max}}$ and the efficiency at maximum power $\eta_{\mathrm{TEG,MP}}$, the latter optimizing the output power density $\dot{w}_{\mathrm{TEG}}$. By definition, $\eta_{\mathrm{TEG,max}} > \eta_{\mathrm{TEG,MP}}$ while $\dot{w}_{\mathrm{TEG}}$ at maximum efficiency is smaller than its maximum possible value for any device where $zT < \infty$. One computes that [17]

$$\eta_{\mathrm{TEG,max}} = \eta_{\mathrm{C}} \frac{\sqrt{1+z\bar{T}}-1}{\sqrt{1+z\bar{T}}+T_{\mathrm{c}}/T_{\mathrm{h}}} \tag{13}$$

where T_{h} and T_{c} are the temperatures at the hot and cold sides, $\bar{T} = (T_{\mathrm{h}} + T_{\mathrm{c}})/2$ and $\eta_{\mathrm{C}} = 1 - T_{\mathrm{c}}/T_{\mathrm{h}}$ is Carnot's efficiency. The pertinent output power density is

$$\dot{w}_{\mathrm{TEG}} = \frac{\sigma_T \alpha^2 (\Delta T)^2}{2\ell} \frac{\sqrt{1+z\bar{T}}}{1+\frac{1}{2}z\bar{T}+\sqrt{1+z\bar{T}}} \tag{14}$$

where $\Delta T = T_{\mathrm{h}} - T_{\mathrm{c}}$ and ℓ is the length of the TE element (often referred to as leg). Maximum efficiency is reached when the ratio between electrical load resistance R_{L} and the TEG resistance r is $m \equiv R_{\mathrm{L}}/r = \sqrt{1+z\bar{T}}$.

Optimizing on $\dot{w}_{\mathrm{TEG}}$ leads instead to the efficiency at maximum power (attained for $m = 1$) [17]:

$$\eta_{\mathrm{TEG,MP}} = \frac{\eta_{\mathrm{C}}}{2}\left(1+\frac{2}{zT_{\mathrm{h}}}-\frac{\Delta T}{4T_{\mathrm{h}}}\right)^{-1} \tag{15}$$

at which $\dot{w}_{\mathrm{TEG}} = \sigma_T \alpha^2 \Delta T^2/(4\ell)$.

While efficiency and power output under the application of a temperature difference are easily computed, in hybrid solar cells TEGs operate under fixed heat flux at the hot side, with the cold side kept either at fixed temperature (Neumann's boundary conditions) or, more realistically, dissipating heat convectively, i.e. following Newton's law (Robin's boundary conditions). In both cases, maximum efficiency and efficiency at maximum power coincide, as in the PV case. Evaluation of efficiency and power output is here more challenging, even under CPA. In a possibly underrated paper, Castro and Happ [18] analysed the first case, assuming an entering heat flux $J_{\mathrm{q,h}}$ with the cold side kept at T_{c}. They found that

$$\eta_{\mathrm{TEG,MP}} = \frac{2m(m-zT_{\mathrm{h}}-1)}{2m^2+(1-2zT_{\mathrm{h}})m+(1+zT_{\mathrm{h}})} \tag{16}$$

where the matching load m is the root of the equation

$$(m-zT_{\mathrm{c}}-1)\left(2m^2+(1-2zT_{\mathrm{c}})m+(1+zT_{\mathrm{c}})\right)-\frac{2z^2}{\alpha^2}\left(J_{\mathrm{q,h}}r\right)=0 \tag{17}$$

and T_{h} follows from $\Delta T = (m+1)(m-zT_{\mathrm{c}}-1)$.

More recently, the problem of the efficiency under constant heat flux has been revisited by Gao Min using a different approach [19], also extending the analysis to more reliable ways to measure zT in real systems—and recovering the very same result as of the efficiency.

Whenever the CPA is relaxed, evaluation of efficiencies becomes more cumbersome and normally require numerical analyses. Quite fortunately, for hybrid solar harvester the CPA is a sensible approximation, at least for the optical concentrations achievable with non-imaging optics. Instead, the impact of contact resistances, both thermal and electrical, should not be neglected, to avoid severe overestimation of efficiencies. Thermal contact resistances partition the applied temperature difference (when the TEG operates across two thermostats) or reduce the temperature difference (when a constant heat flux is applied). On the first count, it could be shown [20] that $\dot{w}_{\mathrm{TEG}}$ is rescaled with respect to its maximum value in the absence of contact resistances $\dot{w}_{\mathrm{TEG,max}}$ as

$$\dot{w}_{\mathrm{TEG}} = \dot{w}_{\mathrm{TEG,max}} \frac{\hat{K}^2}{\left(1+\hat{K}\right)\left(1+z\bar{T}+\hat{K}\right)} \tag{18}$$

where $\hat{K}$ is the ratio between the contact thermal conductance and the TEG thermal conductance. To the best of our knowledge, instead, no analytical model of the role played by contact resistances when TEGs are fed by a constant heat flux is available.

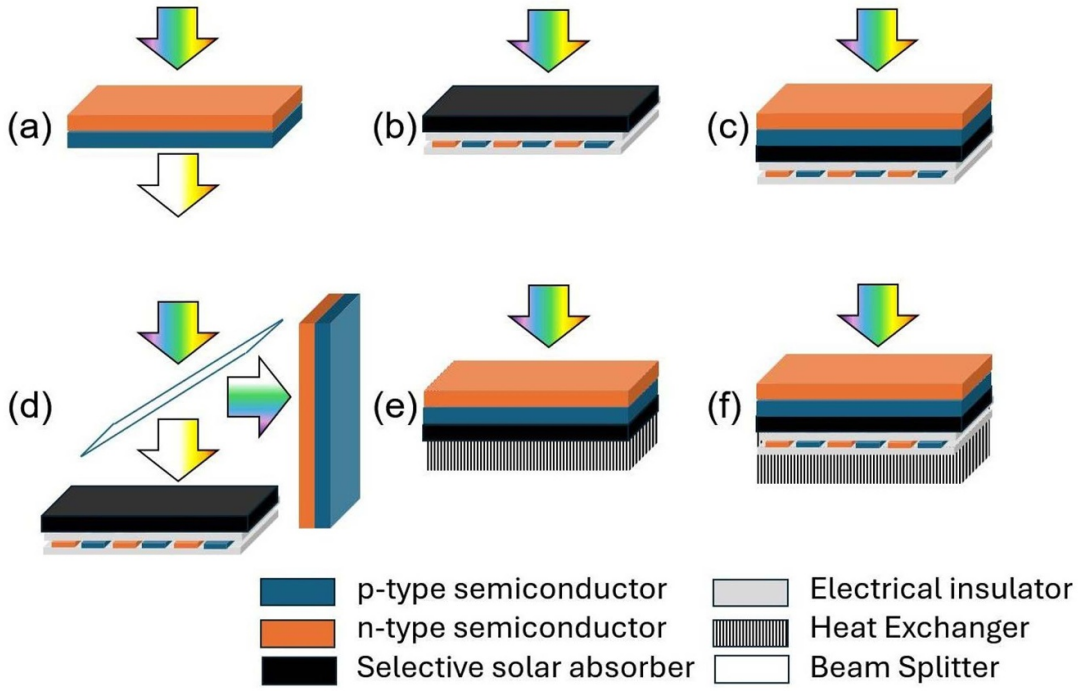

Figure 3. Schematics of the most common solar harvesters: (a) photovoltaic cell; (b) solar thermoelectric generators; (c) tandem hybrid photovoltaic-thermoelectric generator; (d) spectral-split hybrid photovoltaic-thermoelectric generator; (e) hybrid photovoltaic-thermal generator; (f) hybrid photovoltaic-thermoelectric-thermal generator. Each class of device may convert sun with or without the use of solar concentrators.

3. PV-TE pairing strategies

3.1. Nomenclature

As already mentioned, solar harvesting plays a dominant role among renewable power sources. Solar radiative power can be converted into electric power not only using the PV effect but also, in very special situations, using TEs alone—not to mention thermal harvesters, used to obtain heat at temperatures ranging from some tens of degree Celsius (for home heating and sanitary) to more than 3000 °C in solar furnaces. Hyphenated technologies are not limited to pairing PV cells and TEGs, indeed. PV cell may be paired to cyclic engines (mostly running Rankine or Stirling cycles) [21]. As an alternative, heat released by PV cells is often used as such for heating [22]. Furthermore, thermo-PV cells preprocess Sun power, using it to heat a black-body in such a way that the re-emitted radiation is peaked at the energy gap of a PV cell, converting therefore radiation with the highest efficiency. Often, low-temperature heat they release is fed to TEGs or to cyclic engines for additional conversion or to a heat exchanger to produce hot water [23].

Such an extended set of technology has led to a rather confusing nomenclature, especially for the hybrid (hyphenated) harvesting strategies. In this review we will refer to harvesters generating power by using a TEG stage only as solar TEGs (STEGs) while reserving the name of PV-thermoelectric (PV-TE) solar generators to harvesters where a PV cell and a TEG are used, either in parallel or in series. When a third thermal stage is added, trigeneration systems will be referred to as PV-thermoelectric-thermal (PV-TE-Th) generators. Finally, PV-thermal (PV-Th) Generators will refer to PV cells discharging heat toward a convective heat exchanger, either directly or through a storage tank (figure 3).

STEGs have been the subject of a recent review [24] and will not be covered in this paper. Suffice here to say that, although of great conceptual interest, they pay in full the still low efficiency of TE materials, converting Sun power with maximum efficiencies of $\approx 7.4\%$ [25]. Currently, their applicative interest is limited to contexts where PV cells cannot be conveniently deployed due to atmospheric conditions (snow, sandstorms) that would require continuous maintenance. Instead, pairing TEGs to PV cells is disclosing realistic opportunities of efficiency enhancement, and will be the focus of the review—with a special attention to silicon-based PV cells and modules, due to their dominant share in the solar market.

3.2. Tandem PV-TE generators

In a tandem PV-TE generators (figure 3(c)), the TE stage is placed in contact with the back of the PV cell through a blackbody, often referred to as selective solar absorber (SSA). The concept behind this layout is that the portion of the solar spectrum not absorbed by the PV cell is collected and converted into heat by the SSA. It adds on the heat released by the PV cell due to thermalisation of hot carriers and to other parasitic sources of losses degrading electric power. The overall heat flux enters then the TE stage, where it is partially converted into electric power—the unconverted heat being then either released to the surroundings or used to warm sanitary water [26]. In this way, all the heat withdrawn from the PV cell is fed to the TEG. Furthermore, the hybrid harvester layout is simple, not requiring but the SSA and the TEG as additional components. This makes hybridisation of existing PV cells and modules feasible by retrofitting the solar device, with marginal labour and costs. However, the design of tandem PV-TE harvesters must account for the opposing needs of the two stages. On one side, the PV stage should be kept at the lowest possible temperature, as long as $\beta_{PV} < 0$, while TEGs should desirably operate over the largest temperature difference to achieve the largest efficiency. Detailed analyses of these contrasting requirements were extensively reported and commented upon in the literature [17, 27–29].

3.3. Spectral-split PV-TE generators

In spectral-split PV-TE generators (figure 3(d)), the solar spectrum is split into two parts, forwarding its portion with photon energy larger that E_g to the PV cell and the remaining part to the SSA for converting it into heat, to be supplied to the TEG. In this way, the two stages are thermally independent, i.e. their temperatures can be independently set to fulfil stage optimality—low temperature for the PV cell, high temperature at the TEG hot side. Although completely evading the conflicting temperature requirements of tandem PV-TE generators, in spectral-split hybrid harvesters the heat generated by thermalisation of hot carriers remains unused, therefore reducing the extra-power generated by hybridisation. Furthermore, the geometry of the overall system is way more complex and expensive than in tandem PV-TE systems, as, in principle, it requires a beam splitter (with its mounting) and an additional heat exchanger to keep TEG cold side and the PV cell as close as possible to room temperature. Finally, re-engineering of existing PV modules by retrofitting is quite doubtable. For a detailed analysis of the energetic profitability of spectral-split PV-TE generators the Reader may refer to references [30–32].

3.4. Other classes of PV-TE generators

Thermoelectric devices may be used not only to collect unused solar power but also to cool down the PV cell, thus raising its efficiency. Use of (powered) Peltier coolers was introduced in 2013 by Najafi and Woodbury [33], who computationally showed a possible increase of the net power output. The advantage was computed to be about 3% in GaAs PV cells operating under 50-Sun concentration [34] and experimentally validated in $GaInP_2$/GaAs/Ge triple-junction solar cells at 1000 suns to be $\approx 4\%$ [35]. More recently, Peltier cooling was analysed coupling the TE device to a commercial Si panel at 1 Sun [36]. A smaller increase of net efficiency by 1%, from $\approx 16\%$ to $\approx 17\%$, was reported.

Along another avenue, trigeneration could be considered, with PV-TE-Th harvesters where the heat released by TEG at its cold side is used to warm up water or other fluids for sanitary or building heating. While pairing of a thermal stage in a tandem PV-TE system adds an additional unbearable constraint in the thermal chain [17], trigeneration could be a viable option in spectral-split PV-TE harvesters.

4. Energetic profitability of PV-TE generators

4.1. Tandem PV-TE generators

Detailed analyses of how contrasting thermal requirements limit the energetic profitability of hybridisation have been the subject of a large number of papers, both theoretical/computational and experimental. In all of them, the focus is on the interplay among the electronic structure of the PV material, the figure of merit of the TEG, and the performances of the heat exchanger dissipating the heat flux leaving the TEG. For tandem PV-TE generators, there is a rather unanimous accordance about the advantage that hybridisation achieves when pairing state-of-the-art TEGs (with $zT \approx 1$ around room temperature) with low ERE and/or large gap PV materials [7]. Not surprisingly, tandem layouts are also found to lead to a higher efficiency when TEGs are paired with perovskite cells in the temperature range where $\beta_{PV} > 0$. Conclusions about mature PV materials (ERE = 0.01–0.001) with lower energy gap—and specifically about Si—are instead more largely divergent, with scholars either reporting (often

small) advantages in terms of power output [37–39] or concluding about the inconvenience of tandem hybridisation [40, 41].

Zhang *et al* [37] systematically compared singe-crystalline (sc) and thin-film polycrystalline Si cells, with power conversion efficiencies (PCEs) of 14.5% and 8.2% under standard testing conditions (STC) (298 K, 1 Sun) tandem-paired to a TEG modelled beyond the CPA and with a figure of merit of 1.2 at 300 K. By optimizing on the heat transfer coefficient h_{HX} of the heat exchanger at TEG cold side, a small improvement of the net efficiency (accounting for the power consumed by forcing the refrigerating fluid) was computed for sc-Si (from 17.5% to 17.7% at 16 suns with $h_{HX} = 1150$ W m^{-2}K) while for thin films the improvement was larger (from 11% to 14% at 12 suns with $h_{HX} = 1000$ W m^{-2}K). An increased efficiency was also reported by Lin *et al* [38] by numerically simulating the tandem pairing of a commercial Si PV cell (PCE = 11.86%) with a commercial Bi_2Te_3-based TEG module, also accounting for thermal contact resistances. Upon electric load matching and optimization of the TEG geometry, a total efficiency for the hybrid system of 13.6% was computed. Rezania *et al* [42] computationally compared the efficiency of PV cells and tandem PV-TE solar harvesters, also accounting for heat dissipation by natural or forced convection and radiation from both the front and rear surfaces of the panels. Solar irradiance at various locations were used. A PCE for the PV cell around 16% was estimated, along with an increase of efficiency upon hybridisation around 0.5%.

Reduced efficiency upon pairing of sc-Si PV cells with Bi_2Te_3-based TEGs was instead reported by Narducci and Lorenzi [40], where the critical importance of effective heat dissipation was stressed, reaching however the conclusion that tandem PV-TE cells may improve the conversion rate of existing solar cells based on lower cost PV materials. A comparable analysis was advanced by Dianhong Li *et al* [39] who systematically compared single-crystalline and thin-film polycrystalline Si cells tandem-paired to a TEG with $zT = 1.5$. Using a heat exchanger at the TEG cold side with a heat transfer coefficient $h_{HX} = 5$ W m^{-2}K, the PV cell would correspondingly reach a temperature of 335 K under 50 suns and 440 K under 200 suns. Despite the extreme PV temperature under high solar concentration, largely exceeding the maximum temperature (≈ 350 K) that a Si PV cells can sustain, a detailed balance of heat fluxes led the authors conclude that hybrid harvesters would never deliver higher power than the stand-alone PV cell (STC PCE = 17.2%) at any optical concentration (from 1 to 200 Sun). Instead, for thin-film Si PVs (STC PCE = 10.5%), hybridisation returned an increase of efficiency of 0.5% at 50 suns, and up to 2.7% at 200 Sun—although at a questionably large T_{PV}.

Soltani *et al* [43] experimentally analysed a tandem PV-TE harvester based upon a commercial PV cell with a PCE of 15% coupled with a commercial Peltier cooler [44], withdrawing heat in both the PV and hybrid harvesters by means of a heat exchanger fed with a nanofluid. The on-field comparative test of the PV cell vs the hybrid displayed an average increase of efficiency by about 1%. A completely different outcome was reached by Yin *et al* [41] with the comparative simulation of tandem hybridised PV-TE harvesters, ruling out any efficiency advantage up to 20 suns either with sc-Si and thin-film polycrystalline Si PV cells (STC PCE of 17.2% and 10.2%, respectively) due to the additional thermal resistance opposed to heat dissipation by the TEG stage.

To find a rationale in such contrasting results we display the reported increase of efficiency in Si-based tandem PV-TE cells as a function the efficiency of the pertinent non-hybridised PV cell (figure 4(a)). A linear decrease of the energetic advantage of hybridisation upon increasing η_{PV} is found. This is not surprising. Tandem hybridisation using relatively low-efficiency PV cells causes a larger amount of heat to be conveyed to the TEG stage, making its contribution to the total output power density more significant. At the same time, however, PV efficiency is further reduced by increasing T_{PV}. This second effect prevails over the advantage of TE heat recovering with high-efficiency PV stages only. In a simplistic analysis, the output power densities delivered by the PV and TEG stages account respectively to $\gamma G_{Sun}\eta_{PV}$ and $\gamma G_{Sun}(1-\eta_{PV})\eta_{TEG}$, where G_{Sun} is the integrated solar irradiance (≈ 1000 W m^{-2} at AM1.5). Thus, since $\eta_{PV} = \eta_{PV}^{(0)}(1+\beta_{PV}(T_{PV}-T^{(0)}))$ (where $\eta_{PV}^{(0)}$ is the PCE at $T^{(0)}$ =298 K), one easily computes that the range of β_{PV} values leading to an increase of power output strictly depends on the efficiency of the non-hybridised PV cell. Thus, moving from a state-of-the-art (PCE = 25%) to a low-quality (PCE = 15%) Si PV cell increases the β_{PV} threshold value by a factor two, making the hybrid solar cell competitive toward the stand-alone PV cell (figure 4(b)). Overall, this quite suggests that the claimed energetic profitability of tandem PV-TE Si-based solar cells mostly originates from the notably low PCEs of the cells used in the experimental or computational studies, confirming the unsuitability of tandem hybridisation for high-quality Si PV cells at current TE efficiencies. Disadvantages of tandem PV-TE over Si-based PV cells when no specific strategy is implemented to compensate for the PV efficiency loss due to overheating has been recently confirmed experimentally [45], and was shown not to

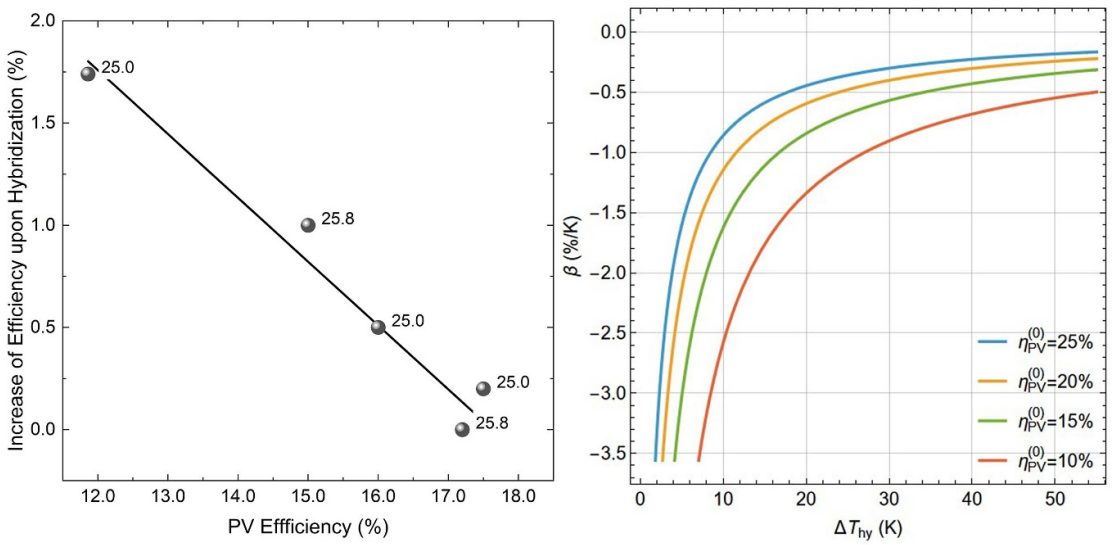

Figure 4. (a) Reported increases of efficiency for Si-based tandem PV-TE cells as a function the efficiency of the pertinent non-hybridised PV cell. Figures labelling data points report the world-record of crystalline Si-based PCE in the year of publication; (b) Threshold values of the temperature coefficient of efficiency as a function of the increase of the PV cell temperature ΔT_{hy} due to its tandem pairing with a TEG stage for various values of the PV cell efficiency under standard conditions (298 (K).

be significantly improved by improving thermal contact resistances through any choice of thermal interface materials [46].

4.2. Spectral-split PV-TE generators

Differently from tandem harvesters, in principle spectral-split PV-TE harvesters are always energetically profitable, as the recovery of the low-energy portion of the solar spectrum adds upon the power output of the PV cell, independently from the TEG efficiency [47]. The critical part of the device in this case is the beam splitter, which should partition the solar spectrum sending to the PV cell only photons with $E > E_g$ while conveying the remaining part of the spectrum to the solar selective absorber in contact with the TEG—without absorbing any part of it. This explains why, over the last decade, most of the activity carried out on this class of PV-TE solar converters has been focused on the development of efficient spectral splitting technologies.

Skjølstrup and Søndergaard [48] compared the use of a lens and of a reflector along with a beam splitter in a concentrated spectral-split PV-TEG, with the aim of evaluating the effect of the light angular distribution on the conversion efficiency. For the splitter, a multilayer was designed and built, with an outer layer made of MgF_2 followed by a variable number of blocks with alternating layers of SiO_2 and Si_3N_4 of different thickness. The whole structure was deposited on a glass substrate. Using the admittance transfer matrix method the authors could optimize the splitter transmittance and reflectance in the pertinent spectral ranges. Experiments carried out on a microcrystalline Si PV cell (PCE = 17.47%) reported that a quarter-wave-layer structure, while ensuring efficient reflectance from 1054 nm to 2500 nm (toward the PV cell), also led to efficient reflection between 351 and 833 nm, where instead full transmission (toward the TEG) would have been desirable. A better spectral partitioning could be achieved by reverting TEG and PV, namely having the TEG collect reflected light and the PV collect the transmitted light. With the beam splitter engineered to work as a high-wavelength-pass filter and upon removal of the (absorbing) MgF_2 front layer, a 162-layer beam splitter let obtain a total efficiency of 19.77%.

The role of the beam splitter was also analysed by Yang *et al* [49], using a commercial multilayer film structure along with a Fresnel lens for the optical concentration, which was set to 146 suns. Silicon PV cell and TEG were kept in contact with a forced convection heat exchanger, using water as the refrigerating fluid at a flowrate of 3.1 l/min—so to keep PV and cold side TEG temperature around 15 °C. Therefore, large temperature differences across the TEG were obtained, ranging between 65 and 160 K, depending on the beam splitter cutoff wavelength λ_c. Regarding the PV cell, optimal λ_c was found to be 1100 nm, when the power output is almost the same as when a mirror is used to reflect the whole beam toward the PV cell. However, such a cutoff wavelength largely reduced the TEG contribution, leading to a marginal increase of the total power production compared to the PV cell alone. Choosing instead a λ_c

Table 1. Summary of performance data upon hybridization. In the table, the following abbreviations were used: TF = thin film; sc = single-crystalline; pc = polycrystalline; location = variable solar irradiance during tests, dependent upon geographical/weather conditions; *n/a* = not available; MOC = maximum operative conditions, i.e. $T_{PV} \leqslant 358$ K. Where the heat transfer coefficient was indicated as 'variable', data refer to the best (highest) efficiencies achieved with the hybrid harvester.

Year	STC PCE (Stand-alone)	PCE (Stand-alone)	PCE (Hybrid)	Optical Conc.	TEG zT @ 300 K	Heat transfer Coefficient ($W\,m^{-2}K$)	Reference
Tandem							
2014	14.5% (bulk, sc)	17.5%	17.7%	16 Sun	1.2	1150	[37]
	8.2% (TF, pc)	10.5%	12.0%	12 Sun	1.2	1000	
2015	11.86% (bulk, sc)	11.86%	13.6%	1 Sun	≈ 1	31.6	[38]
2016	*n/a*	$\approx$ 16%	$\approx$ 16.5%	location	≈ 1	*n/a*	[42]
2017	17.2% (bulk, sc)	18.4%	15.7%	50 Sun	1.5	5	[39]
		18.3%	11.7%	200 Sun	1.5	5	
	10.5% (TF, pc)	11.2%	11.0%	50 Sun	1.5	5	
		11.3%	13.0%	200 Sun	1.5	5	
2017	15.0% (bulk, sc)	12.2%–14.7%	13.5%–15.5%	location	≈ 1	variable	[43]
2017	17.2% (bulk, sc)	19.8%	18.1%	12 Sun	≈ 1	variable	[41]
	10.2% (TF, pc)	12.4%	11.5%	12 Sun	≈ 1	variable	
Spectral-Split							
2016	17.47% (bulk, sc)	17.47%	19.77%	1 Sun	(eff: 4%–8%)	*n/a*	[48]
2023	13.2% (bulk, sc)	13%	9.0%	MOC	≈ 1	Natural convect.	[50]
2024	*n/a*	(1.1 W)	(1.64 W)	146 Sun	≈ 1	PV & TEG cold side @ 288 K	[49]

of 880 nm turned out to maximize the total converted power. Although neither efficiency or power density were reported, the authors claimed an increase of power by 0.22 W, from 1.1 to 1.64 W, gross of the power required by the heat exchanger.

Use of a dichroic mirror was evaluated by Kandil *et al* [50] in a spectral-split concentrated PV-TE solar converter. A Fresnel lens was used to obtain optical concentrations up to 18 suns, set in such a way that the Si PV cell were not exposed to temperatures exceeding 85 °C. This provides different limits for the maximum affordable optical concentration, which is larger when a beam splitter is used. Overall, authors could obtain higher power outputs from PV-TE systems (up to 1215 $W\,m^{-2}$) compared to PV alone (delivering a power density of 900 $W\,m^{-2}$) although the efficiency of the PV-TE converter is lower than in non-hybridised PV cells (9.0% vs 13%).

Overall, even recent investigation confirmed the energetic profitability of spectral-split PV-TE hybrid harvesters. Enhancements of efficiency of some percent when using Si solar cells should be considered remarkable, since Si-based PV cells progressed their PCE by just 1.1% over the last decade. However, their exploitation is possibly severely limited by their economic profitability, as will be discussed in details in the forthcoming section—at least when small solar concentrations are considered.

A summary of the energetic profitability of both tandem and spectral-split PV-TE generators is displayed in table 1.

5. Economic profitability of PV-TE generators

5.1. Tandem PV-TE generators

For tandem Si-based PV-TE generators, it is manifestly not profitable to develop hybrid solar harvesters when no energetic advantage is achievable. Nonetheless, since, as shown, margins of energetic convenience have been reported when coupling low-efficiency Si solar cells with TEGs, an evaluation of their economic profitability is in order. Narducci and Lorenzi [16] outlined a scheme of analysis based upon the physical properties of the PV material to evaluate the eventual economic viability of tandem PV-TE solar harvesters. The model assumed a PV-TE device made of a PV cell in contact with the TEG through the SSA, acting as a perfect black body. Furthermore, it was assumed that the whole device is suitably encapsulated, preventing convective heat dissipation, and that radiative dissipation from the PV cell is fully blocked by a suitable heat mirror, namely a coating covering the PV cell side facing the Sun and fully back-reflecting the electromagnetic radiation emitted by the PV cell at T_{PV} while transmitting all solar radiation [51]. No thermal contact resistance was considered either. Overall, such assumptions

make the model *overestimate* its performances with respect to a real tandem PV-TE harvester. Therefore, the model provided a no-go criterion, in the sense that no hybrid tandem PV-TE generator reporting an economic convenience index EcCI, defined as the ratio between the cost per watt of the PV-TE cell and of the stand-alone PV cell, smaller than one justifies the hybridisation of the pertinent PV cell. Taking an ERE of $< 10^{-6}$ for a Si PV cell (PCE $< 18\%$), an EcCI> 1 is found at 1 Sun, which further increases even at moderate concentrations (5 suns). No economic viability is instead reported for state-of-the-art Si solar cells (ERE $= 10^{-3}$—10^{-2}) for realistic zT values (around 1 at room temperature). Regarding the PayBack period (PBP), namely, the period of time needed to recover capital costs, true PBPs (neglecting taxation and other supporting benefits) were estimated to be around 25–30 years for both domestic and industrial conventional solar power plants [52]. In hybrid harvesters, PBPs scale with EcCI and with the ratio of PV-TE to PV capital costs. However, even in the case of concentrated solar cells, this leads to an increase of PBP—although of less than 5%. Since TEGs are known to have a very extended lifetime, much larger than that of the solar cells, hybridisation retains acceptable PBPs even in the absence of favourable taxation. Therefore, EcCI remains the critical key parameter ruling affordability of tandem hybridisation.

It should be stressed that, still today, the capital cost of TEGs is largely dominated by heat exchangers [53]. Heat exchanger technologies remain largely based on (micro)mechanical machining, leading to high costs per dissipated power density, and their cost impacts profitability of *any* TE device (either harvesters or coolers) [54, 55]. Since heat dissipaters are already mounted in concentrated PV solar cells, even at modest concentrations (5 suns), this drives EcCI to more favourable values for roof-top concentrated PV-TE harvesters. Indirect additional evidence of the prospects provided by optical concentration comes from highly concentrated (100–1000 suns) tandem PV-TE systems [56, 57]. However, in all cases high-performance (typically triple-junction) solar cells are preferred over Si.

5.2. Spectral-split PV-TE generators

We anticipated that economic convenience of spectral-split PV-TE generators is critical. While energetic convenience is proved, the extra capital costs of the device make careful and realistic analyses of power costs especially important, largely explaining the number of papers even recently published on the topic. It is however unfortunate that some of such studies were spoiled by often overoptimistic estimates of the energetic advantage due to spectral-split hybridisation.

Focusing also in this case on Si-based harvesters, an accurate analysis was reported by Babu and Ponnambalam [58] for different implementations of the spectral-split concept. In no case was a lower levelised cost of energy (LCoE) found for hybrid harvesters, with increases of LCoE ranging between 8.7% and 90% compared to stand-alone PV cells. However, with energy gains comprised between 10% and 50%, the PBP was estimated to scale down from 20–25 years to 15–20 years. Comparable conclusions were reached by Moshwan *et al* [59], who remarked how the commercialization of any type of PV-TE solar converters (and the consequent additional development of more effective hybrid cells) still must rely on incentives and subsidies. The conclusion drastically changes moving to multiple junction solar cells operating at high optical concentrations, where the complexity of the hybrid cell mounting and the costs of the additional optical components is compensated by the larger heat flux converted over larger temperature differences by the TE stage [60, 61]. Furthermore, since even non-hybridized multiple junction solar cells require active heat dissipation, clever design of PV-TE system lets a single heat exchanger service both the PV and the TE stages, avoiding cost duplication [60] and therefore further lowering LCoE of hybrid harvesters.

In summary, at the current state of the art, solar-split PV-TE solar harvesters appears as the most promising hyphenated solar conversion efficiency, whose technological readiness is not hampered by hard-to-overcome physical constraints. Improvements of the quality of optical components, possibly coupled to abated fabrication costs, could let it reach competitive LCoE. Yet, high optical concentrations, structural complexity and hightened capital costs seem qualify them for solar parks and large power installations more than for distributed, roof-top solar power generation.

6. Prospectives on the hybridisation of Si-based PV cells

Based upon the analyses of energetic and economic convenience of silicon-based PV-TE hybrid harvesters, one might conclude that recovering the heat left unconverted by stand-alone PV cells is always unprofitable. In tandem PV-TE systems, the opposite thermal needs of the PV and the TE stages makes

impossible to obtain an overall increase of the conversion efficiency due to the largely negative coefficient of temperature of the PV efficiency of high-quality Si cells, either single-crystalline or polycrystalline. On the other side, when a spectral-split geometry is chosen, the increase of efficiency cannot compensate for the larger capital cost of the harvesters, making the LCoE higher although reducing its PBP compared to stand-alone solar cells. Although such conclusions are proper, quite explaining why most of the research effort on hybrid solar harvesters have addressed III–V multiple junction solar cells at high solar concentrations [62], perovskite-based [53, 63] or, recently, perovskite-silicon double junction solar cells [10], nonetheless they should not be taken as final as they might appear. TEGs with higher efficiency around room temperature, possibly making use of more geo-abundant, less expensive materials than tellurides, will surely narrow the efficiency gap in tandem devices and the cost gap in spectral-split systems [64]. Additionally, module scale-up would lessen capital costs. However, even in the lack of novel materials, creative approaches might positively affect the energo-economic balance of PV-TE harvesters.

Novel approaches to overcome the contrasting thermal requirements of the two stages have been recently advanced. Already in 2016 Li *et al* [65] proposed to thermally decouple the PV and TEG stages, still in a tandem geometry, by introducing a microchannel heat pipe collecting heat from the PV back and transferring it to the TEG hot side. Efficiency was found to exceed that of the stand-alone PV cell for solar irradiances ranging from 0.15 to 1 Sun, with the improvement increasing with the irradiance up to $\approx 2\%$. Additionally, although the conventional tandem PV-TE harvester delivered a higher power, authors claimed that the novel system was more economically viable, as it required smaller TEGs. In this line, Zhou *et al* [66] proposed and experimentally validated an approach based on a fluid collecting the infrared portion of the solar spectrum, preventing it from reaching the PV cell. The hot fluid is used for heating while the electric power is mainly generated by the PV cell, with the TEG stage, in thermal contact with the back of the PV cell, collecting and converting the heat released due to non-radiative recombination in the PV device. This strategy keeps the PV cell at lower temperature, preventing the degradation of its efficiency, although at the cost of a very minor contribution of the TEG to the total electric power. Furthermore, the geometry avoids the extra cost of the beam splitter. As stressed by the authors, many system components play a key role setting the device efficiency and its possible advantage with respect to the stand-alone PV cell. This includes the transparency and reflectance of the windows used in the chamber through which the fluid circulates, the fluid itself, acting as the solar splitter, and the thermal interface material used at the PV-TEG contact. Despite the extensive effort to optimize all components, the device (using water as the fluid, a sc-Si PV cell and a commercial Bi_2Te_3 TE stage) could provide higher power outputs compared to the standard tandem PV-TE device (with no absorbing fluid) but could not compete with the stand-alone PV cell. Yet, the thermal portion of this trigeneration technology could be considered as an advantage, beyond electric power generation.

This concept was experimentally validated again in 2023 by Zhang *et al* [67] who further perfected the idea by introducing a three-way valve addressing the heat released by the PV stage, still a sc-Si PV cell (PCE $\approx 15.5\%$), toward either side of the TEG. The idea was to retain its polarity while generating power when the surroundings were either at higher or lower temperature than the PV cell, depending on the season. Experiments extended over a whole year in Wuhan, PRC, reported an encouraging increase of the efficiency at maximum power from 21.2% to 22.6%.

As a comparison, Wei Li and coworkers [68] reconsidered the possibility of collecting the low-frequency portion of the solar spectrum before it reached the sc-Si PV stage (with a very low PCE of 14%) using what was re-named an 'optical filter', namely a transparent multi-channelled layer where water could absorb the IR solar spectral portion along with the heat released by the PV cell, conveying it to a phase-change material in contact with the TEG hot side. This design would minimize the PV heating while keeping the TEG hot side at a relatively high temperature. Computations predicted an increase of efficiency up to 8%, from 14% to 22%. No experimental validation of such estimate could be provided, however.

Other innovative layouts were also recently advanced. Use of phase-change materials as thermal batteries to (partially) decouple PV and TEG stages in tandem geometry is raising increasing interest [69]. Optimization of TEG geometry also proved relevant to tandem PV-TE systems. The making of dedicated TE modules, with unconventional length to cross-section leg ratios, has been widely assessed to enhance TEG power generation [70]. More recently, scholars explored the use of non-cuboid (e.g. hourglass, truncated pyramid) leg shapes, namely TE legs whose cross-sectional area changes along their height [71–73]. Such an ingenious expedience lets locally increase the leg thermal resistance, resulting in higher power outputs. Replacing heat exchangers with evaporation systems, where the heat released at the TEG cold side is dissipated by evaporation in a solar still, suggests an alternate type of solar trigeneration,

with the additional advantage that heat withdrawal no longer implies power consumption (by the forced fluid convection through the heat exchanger), becoming instead instrumental to freshwater production [74].

7. Summary and conclusions

In this paper, the state of the art of research about the recovery of heat from single-junction solar cells by using TEGs has been reported and discussed. The focus of the paper was on Si-base solar cells, since they cover the overwhelming majority of PV cells currently deployed, with a major role in the distributed production of electric power. It was shown how the technological maturity reached by Si solar cells makes all challenges in the making of energetically and economically convenient hybridization of solar harvesters even more critical. At the same time, however, certified and reproducible increases of efficiency even of just a few percent would have a tremendous impact on solar harvesting and on the application of paired PVs and TEGs. We found that conventional tandem PV-TE pairing confirmed its inconvenience from the energetic point of view. Instead, the spectral-splitting approach still runs into limitations concerning capital costs, causing higher LCoE, along with a structural complexity that hinders its deployment in distributed, roof-top solar harvesters. Beyond the favourable contribution that will come from improved TE materials, overcoming nowadays efficiency limitations as well as raw material costs and availability, recent research reports have shown how there is still quite a bit of room available to achieve hybridization profitability by working on system geometry, extending tandem and spectral-splitting concepts beyond their standard implementation, possibly shortening the path toward successful full-spectrum conversion of solar power.

Funding

A.M. acknowledges the support received by the European Union–NextGenerationEU, Mission 4, Component 2.

Data availability statement

All data that support the findings of this study are included within the article (and any supplementary files).

Author contributions

Dario Narducci 0000-0002-3307-1070
Conceptualization (lead), Formal analysis (lead), Funding acquisition (lead), Writing – original draft (lead), Writing – review & editing (equal)

Federico Giulio 0009-0007-0870-7595
Data curation (equal), Visualization (equal), Writing – review & editing (equal)

Antonio Mazzacua 0009-0005-8079-5564
Data curation (equal), Visualization (equal), Writing – review & editing (equal)

References

[1] International Energy Agency (IEA) 2025 *Renewables 2025* (available at: www.iea.org/reports/renewables-2025)
[2] Philipps S, Warmuth W, Bett A, Burger B, Kost C, Neuhaus H, Nold S, Preu R, Reichel C and Rentsch J 2025 Photovoltaics report (available at: www.ise.fraunhofer.de/content/dam/ise/de/documents/publications/studies/Photovoltaics-Report.pdf)
[3] Green M A, Dunlop E D, Yoshita M, Kopidakis N, Bothe K, Siefer G, Hao X and Jiang J Y 2025 *Prog. Photovolt., Res. Appl.* **33** 3–15
[4] Shockley W and Queisser H J 1961 *J. Appl. Phys.* **32** 510–9
[5] Ballif C, Haug F J, Boccard M, Verlinden P J and Hahn G 2022 *Nat. Rev. Mater.* **7** 597–616
[6] Huen P and Daoud W A 2017 *Renew. Sustain. Energy Rev* **72** 1295–302
[7] Li G, Shittu S, Diallo T M, Yu M, Zhao X and Ji J 2018 *Energy* **158** 41–58
[8] Wei X, Zhang P, Xu T, Zhou H, Bai Y and Chen Q 2022 *Chem. Soc. Rev.* **51** 10016–63

[9] Kandil A A, Salem M S, Awad M M and Sultan G I 2023 *Adv. Sustain. Syst.* **7** 2300012
[10] Alghamdi H A, Maduabuchi C C, Okoli K, Alobaid M, Alghassab M A, Alsafran A S, Makki E A and Alkhedher M A 2024 *Int. J. Energ. Res.* **2024** 1050785
[11] Hirst L C and Ekins-Daukes N J 2011 *Prog. Photovoltaics Res. Appl.* **19** 286–93
[12] Dupré O, Vaillon R and Green M A 2015 *Sol. Energy Mater. Sol. Cells* **140** 92–100
[13] Dupré O, Vaillon R and Green M 2016 *Thermal Behavior of Photovoltaic Devices: Physics and Engineering* (Springer)
[14] Green M A 2012 *Prog. Photovolt., Res. Appl.* **20** 472–6
[15] Nelson J 2003 *The Physics of Solar Cells* (World Scientific Publishing Company)
[16] Narducci D and Lorenzi B 2021 *ACS Appl. Energy Mater.* **4** 4029–37
[17] Narducci D, Bermel P, Lorenzi B, Wang N and Yazawa K 2018 Hybrid photovoltaic-thermoelectric generators: materials issues *Springer Series in Materials Science* vol 268 (Springer)
[18] Castro P S and Happ W W 1960 *J. Appl. Phys.* **31** 1314–7
[19] Min G 2022 *Energy Environ. Sci.* **15** 356–67
[20] Apertet Y, Ouerdane H, Glavatskaya O, Goupil C and Lecoeur P 2012 *EPL (Europhys. Lett.)* **97** 28001
[21] Loni R, Mahian O, Markides C N, Bellos E, le Roux W G, Kasaeian A, Najafi G and Rajaee F 2021 *Renew. Sustain. Energy Rev* **150** 111410
[22] Vengadesan E and Senthil R 2020 *Sol. Energy* **206** 935–61
[23] Gamel M M A, Lee H J, Rashid W E S W A, Ker P J, Yau L K, Hannan M A and Jamaludin M D Z 2021 *Materials* **14** 4944
[24] Manghwar R, Selvaraj J, Abd Rahim N, Kumar L and Khoharo H 2024 *Appl. Therm. Eng.* **257** 124231
[25] Kraemer D, Jie Q, Mcenaney K, Cao F, Liu W, Weinstein L A, Loomis J, Ren Z and Chen G 2016 *Nat. Energy* **1** 16153
[26] Li H, Zhang H, Li Y, Zhang W, Zhang L, Niu X, Li Y and Hong W 2025 *Energy* **321** 135483
[27] Park K T *et al* 2013 *Sci. Rep.* **3** 2123
[28] Lorenzi B, Acciarri M and Narducci D 2015 *J. Mater. Res.* **30** 2663–9
[29] Contento G, Lorenzi B, Rizzo A and Narducci D 2017 *Energy* **131** 230–8
[30] Imenes A and Mills D 2004 *Sol. Energy Mater. Sol. C.* **84** 19–69
[31] McCambridge J D *et al* 2011 *Prog. Photovolt., Res. Appl.* **19** 352–60
[32] Sibin K, Selvakumar N, Kumar A, Dey A, Sridhara N, Shashikala H, Sharma A K and Barshilia H C 2017 *Sol. Energy* **141** 118–26
[33] Najafi H and Woodbury K 2013 *Sol. Energy* **91** 152–60
[34] Kil T H *et al* 2017 *Nano Energy* **37** 242–7
[35] Teffah K and Zhang Y 2017 *Sol. Energy* **157** 10–19
[36] Eid A F, Lee S, Hong S and Choi W 2022 *Sol. Energy* **245** 254–64
[37] Zhang J, Xuan Y and Yang L 2014 *Energy* **78** 895–903
[38] Lin J, Liao T and Lin B 2015 *Energ. Convers. Manage.* **105** 891–9
[39] Li D, Xuan Y, Li Q and Hong H 2017 *Energy* **126** 343–51
[40] Narducci D and Lorenzi B 2016 *IEEE Trans. Nanotechnol.* **15** 348–55
[41] Yin E, Li Q and Xuan Y 2017 *Energ. Convers. Manage.* **143** 188–202
[42] Rezania A, Sera D and Rosendahl L 2016 *Renew. Energy.* **99** 127–35
[43] Soltani S, Kasaeian A, Sarrafha H and Wen D 2017 *Sol. Energy* **155** 1033–43
[44] The paper reports an almost surely mistaken zT value of 2.5 at $T = 298$ K for the Peltier cooler (table 2, $z = 0.0085$ K^{-1}). However, this does not impact the experimental results
[45] Yousif H S and Jalil S M 2025 *Int. Commun. Heat Mass* **169** 109843
[46] Shurafa S M A L, Basim Ismail F, Kazem H A, Ee Sann T and Almajali T A H 2024 *Sol. Energy* **273** 112514
[47] Min G 2022 *ES Mater. Manuf.* **16** 13–18
[48] Skjølstrup E and Søndergaard T 2016 *Sol. Energy* **139** 149–56
[49] Yang S, Yin E, Li Q and Long Y 2024 *Appl. Therm. Eng.* **248** 123177
[50] Kandil A, Awad M, Sultan G and Salem M 2023 *Energ. Convers. Manage.* **280** 116795
[51] Fan J C C and Bachner F J 1976 *Appl. Opt.* **15** 1012–7
[52] (Available at: www.nrel.gov/news/detail/features/2022/aging-gracefully-how-nrel-is-extending-the-lifetime-of-solar-modules) (Accessed 11 January 2026)
[53] Narducci D and Lorenzi B 2023 *Jpn. J. Appl. Phys.* **62** SD0801
[54] Hendricks T J, Yee S and LeBlanc S 2016 *J. Electron. Mater.* **45** 1751–61
[55] Hendricks T, Caillat T and Mori T 2022 *Energies* **15** 7307
[56] Ismaila K G, Sahin A Z and Yilbas B S 2021 *J. Therm. Anal. Calorim.* **145** 1035–1052
[57] Rodrigo P, Valera A, Fernández E and Almonacid F 2019 *Appl. Energ.* **238** 1150–62
[58] Babu C and Ponnambalam P 2021 *Sustain. Energy Technol, Assess.* **43** 100932
[59] Moshwan R, Shi X L, Zhang M, Yue Y, Liu W D, Li M, Wang L, Liang D and Chen Z G 2025 *Appl. Energy* **380** 125032
[60] Alnajideen M and Min G 2022 *Energ. Convers. Manage.* **251** 114981
[61] Yin E and Li Q 2023 *Energy* **282** 128294
[62] Guo X, Zhai H, Wu Z, Wang Y and Xie H 2023 *Energy Rep.* **9** 1426–35
[63] Xu L, Xiong Y, Mei A, Hu Y, Rong Y, Zhou Y, Hu B and Han H 2018 *Adv. Energy Mater.* **8** 1702937
[64] Narducci D and Giulio F 2022 *Materials* **15** 1214
[65] Li G, Zhao X and Ji J 2016 *Energ. Convers. Manage.* **126** 935–43
[66] Zhou Y P, Li M J, Hu Y H and Ma T 2020 *Appl. Energ.* **260** 114258
[67] Zhang Y, Zhu N, Zhao X, Luo Z, Hu P and Lei F 2023 *Energy* **274** 127342
[68] Li W, Li Q, Kan J, Zhang Y, Zhao W, Wang J, Zhang X and Zhao J 2025 *Energy* **335** 138058
[69] Hassan F, Jamil F, Hussain A, Ali H M, Janjua M M, Khushnood S, Farhan M, Altaf K, Said Z and Li C 2022 *Sustain. Energy Technol. Assess.* **49** 101646
[70] Shittu S, Li G, Tang X, Zhao X, Ma X and Badiei A 2020 *Energy* **202** 117742
[71] Choo S *et al* 2024 *Nat. Energy* **9** 1105–16
[72] Yang S E, Lee J, Li H, Ryu B and Son J S 2025 *Energ. Environ. Sci.* **18** 8537–48
[73] Zianni X 2025 *J. Appl. Phys.* **138** 165101
[74] Gui J, Li C, Cao Y, Liu Z, Shen Y, Huang W and Tian X 2023 *Nano Energy* **107** 108155